Distributed Divertor Radiation through Convection in DIII-D

A. W. Leonard, M. A. Mahdavi, S. L. Allen,* N. H. Brooks, M. E. Fenstermacher,* D. N. Hill,* C. J. Lasnier,* R. Maingi,† G. D. Porter,* T. W. Petrie, J. G. Watkins,‡ and W. P. West

General Atomics, P.O. Box 85608, San Diego, California 92186-5608

(Received 24 February 1997)

The radiative dissipation of divertor target heat flux on DIII-D is shown to greatly exceed the limitations of energy transport dominated by electron thermal conduction parallel to the magnetic field. More than 80% of the power flowing into the outboard divertor is dissipated through radiation with a broad poloidal profile. It is shown that energy transport dominated by convection over a large region of the divertor is consistent with the data. [S0031-9007(97)03465-0]

PACS numbers: 52.55.Fa

The reduction of tokamak divertor target plate heat flux remains a primary goal of magnetic fusion energy research. The design for the power-plant-sized international thermonuclear experimental reactor (ITER) tokamak requires that ~80% of the 300 MW of alpha-particle heating power be dissipated through radiation before deposition on the divertor plates [1]. Much of this radiation should come from the divertor region to minimize degradation of the core plasma confinement. In addition, it is desirable to distribute the radiation throughout the divertor volume to prevent localized heating of the divertor structure. It has often been argued [2] that divertor energy transport dominated by parallel electron thermal conduction, or $q_\parallel = -\kappa T_e^{5/2} dT_e/ds_\parallel$, leads to severe localization of the intense radiating region along the field lines and ultimately limits the fraction of energy flux that can be radiated before the field lines strike the divertor target. This is due to the strong $T_e^{5/2}$ dependence of electron heat conduction which results in very short spatial scales of the T_e gradient at high power densities and low temperatures where deuterium and impurities radiate most effectively. However, we have greatly exceeded this constraint on DIII-D with deuterium gas puffing which reduces the peak heat flux to the divertor plate a factor of 5 while distributing the radiation throughout the divertor [3]. The uniformity in radiation, shown to be a factor of 2 from the X point to the target plate, is 3 times better than required in the design of the ITER [4]. We find that electron thermal conduction cannot account for the measured distribution of divertor radiation and energy transport. However, plasma convection at the ion sound speed through much of the divertor is consistent with our observations.

The transport of energy parallel to the magnetic field in the scrape-off layer (SOL) can be described by [5]

$$\frac{d}{ds}\left[-\kappa T_e^{5/2}\frac{dT_e}{ds} + n v_\parallel \left\{\frac{5}{2}(T_i + T_e) + \frac{1}{2} m_i v_\parallel^2 + I_0\right\}\right] = S_E, \quad (1)$$

where s is the parallel field line length, κ is the parallel electron thermal conductivity, T_e and T_i are the electron and ion temperatures, respectively, n is the plasma density, m_i is the ion mass, $v_\parallel$ is the plasma fluid velocity parallel to the magnetic field, I_0 is the atomic ionization potential (13.6 eV for a deuterium atom), and S_E represents volume sources and sinks of energy, such as radiation, ionization, neutral collisions, and charge exchange, and Ohmic heating due to any SOL currents. In this formulation we have combined the electron and ion energy and disregarded ion viscosity and perpendicular diffusion of energy. The implications of any perpendicular diffusion will be discussed after presentation and analysis of our data.

The first term in the energy transport equation is electron thermal conduction. Ion conduction is an order of magnitude smaller for $T_i = T_e$ and has been neglected. Conduction, as stated earlier, is often assumed to carry the bulk of the SOL power [6,7] and, as we will show, this is true in typical DIII-D H-mode divertor plasmas with no additional gas puffing. However, with conduction dominated transport of even moderate energy flux densities in DIII-D of $q_\parallel \geq 10$ MW/m^2, T_e will rise above 15 eV in less than 0.5 m of parallel length from the strikepoint. Thus there is only a small region of the divertor available for effective radiation from deuterium and carbon, the dominant impurity in DIII-D. Carbon radiation peaks at $T_e \leq 15$ eV and drops by more than an order of magnitude [8] at $T_e \geq 20$ eV. This problem becomes much worse for the expected higher power densities expected in future divertors.

Convection, the second group of terms in Eq. (1), allows transport of energy without a temperature gradient. Here we have included the ionization potential of the plasma in the convective term because we do not experimentally determine the ionization distribution, an energy sink, nor do we determine the fraction of radiation and target plate heat flux that results from plasma recombination. Instead we combine the competing ionization and recombination terms into a potential carried by the plasma. We will see that in DIII-D convection gives us a mechanism whereby energy is transported through the divertor at lower T_e allowing efficient radiation.

The power flowing through the outboard divertor leg is described by $\nabla \cdot q_\parallel = S_E$ where $q_\parallel$ is the parallel heat flux, the sum of conduction and convection, and S_E,

the plasma volume sources and sinks of energy, is due principally to atomic radiation. The effects of neutral interactions will be discussed after presentation of the data. Ohmic heating in the SOL, a possible source of energy, is ignored as SOL currents [9] of $<50\ \mathrm{kA/m^2}$ are measured for these plasmas and the associated heating represents a small perturbation to overall power balance. For this analysis we treat the SOL below the X point as a 1D plasma as a function of $L_\parallel$, the field line parallel distance to the divertor plate. The plasma radiation, $\varepsilon(L_\parallel)$, is measured by two poloidally separated 24-channel bolometer arrays whose view chords are shown in Fig. 1. The signals from these two arrays are inverted to produce a 2D radiation profile [10], as also shown in Fig. 1. This profile is integrated radially through the divertor SOL and with the assumption of toroidal symmetry produces a 1D profile of radiation, $\varepsilon_{\mathrm{SOL}}(z)$, as a function of distance from the divertor plate. This inversion and subsequent integration agrees well with the 1D profile obtained from the horizontally viewing bolometer chords alone. We calculate the total energy flowing in the divertor, $Q_{\mathrm{tot}}(z)$, by starting with the divertor target heat flux measured by an IR camera [11] and integrating the 1D radiation profile. Contributions from plasma radiation are subtracted from the target heat flux. We finally convert to energy flux density, $q_\parallel(L_\parallel)$, by dividing by the cross-sectional area of the SOL perpendicular to the magnetic field. The SOL area normal to the magnetic field lines is determined by the heat flux width at the divertor plate in conjunction with magnetic equilibrium measurements and remains constant through the divertor assuming constant SOL magnetic flux. The parallel path length, $L_\parallel$, is converted from z by magnetic mapping of a field line in the center of the SOL.

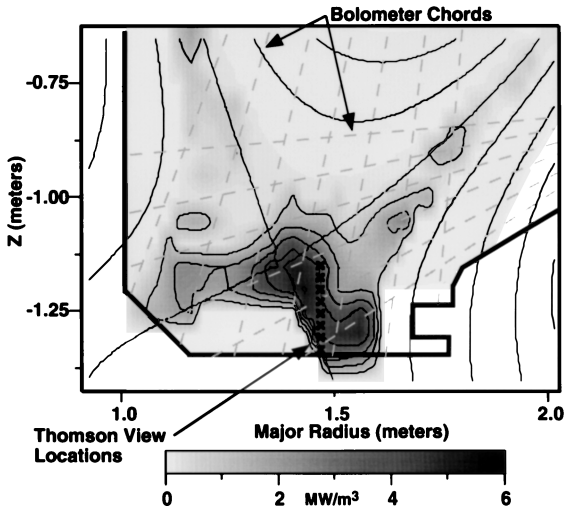

FIG. 1. The 2D radiation profile and divertor geometry for radiative plasmas used in heat transport analysis. Also shown are the bolometer view chords and the divertor Thomson system measurement locations.

To compare our radiating divertor plasmas to the energy transport described in Eq. (1), we use a divertor equilibrium as shown in Fig. 1, which with divertor sweeping allows divertor Thomson scattering (DTS) diagnostic [12,13] measurement of the divertor plasma electron temperature and density along flux surfaces. This X-point location provides three bolometer chords from the horizontal array from the X point to the divertor for adequate spatial resolution of the radiated power for this analysis. We obtain divertor data from ELMing H-mode plasmas with a plasma current of 1.4 MA and safety factor q_{95} of $\sim$4.2 and injected power of about 6 MW. With no gas puffing the $q_\parallel$ profile, determined by the technique described above, is shown in Fig. 2(a). Approximately 40 $\mathrm{MW/m^2}$ flows into the outboard divertor leg below X point with only about $\sim$15% of it radiated before striking the divertor plate. The width of the heat flux at the divertor plate maps to about 1 cm at the midplane. If parallel electron thermal conduction dominates the energy transport then from Eq. (1) we can integrate $q_\parallel = -\kappa T_e^{5/2} dT_e/ds$, where $\kappa = 1.55 \times 10^3$ in eV and mks units for these plasmas, to produce a T_e profile. Integrating from the divertor target with the measured electron temperature of 20 eV near the target we arrive at the conduction-fitted T_e

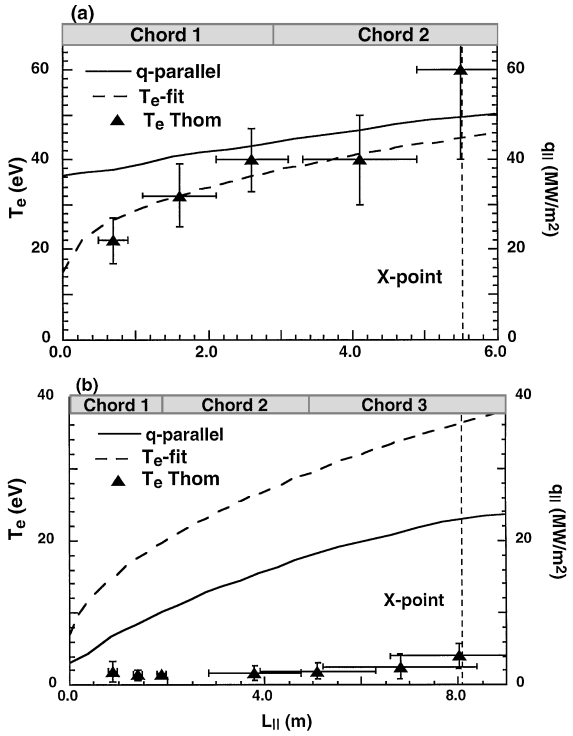

FIG. 2. The outboard divertor energy flux analysis for (a) standard ELMing H mode and (b) radiative divertor through deuterium puffing. Shown are the energy flux profile, $q_\parallel$, the fitted T_e profile for conduction dominated transport, and measurements of T_e from divertor Thomson scattering measurements. Shown at the top of the graphs are the approximate view locations of the horizontal viewing bolometer chords.

profile as plotted in Fig. 2(a). The 20 eV measurement is also consistent with a sheath boundary condition [14] and our measured density and target heat flux. We compare the conduction-fitted T_e in Fig. 2(a) with the T_e profile measured by DTS, averaged over the same SOL width as that used in the $q_{\|}$ calculation. The experimentally measured T_e, increasing from ~20 eV near the target to more than 40 eV at the X point, is seen to be consistent with that inferred from conduction dominated energy flux. The density varies from $\sim 0.5 \times 10^{20}$ m^{-3} at the divertor target to $\sim 0.3 \times 10^{20}$ m^{-3} near the X point.

Such good agreement cannot be obtained in our highly radiating divertor plasmas. With strong deuterium puffing, ~100 Torr l/s, we produce intense divertor radiation and reduce peak divertor plate heat flux by a factor of 3–5, or a factor of 5–10 if we subtract the contribution of radiative heating of the target plate. The reduced heat flux can be maintained with little or no effect on the core plasma confinement with proper tailoring of the gas puff. Further details of this mode of divertor operation can be found in Ref. [15]. The energy transport in the divertor under these conditions is summarized in Fig. 2(b). Approximately 25 MW/m^2 of power flows into the divertor below the X point, of which almost 85% is radiated away before reaching the divertor plate. The spatial resolution of the radiation measurement is given by the views of the horizontal bolometer array shown at the top of the figure. The lower initial energy flux into the divertor is due to a wider SOL width at the divertor plate for these plasmas and a small increase in radiation above the X point. The predicted T_e profile required to support the energy flux through conduction is also plotted in Fig. 2(b). Even for the modest energy flux at the divertor plate for these conditions T_e must rise above 15 eV in a relatively short parallel distance of $\leq$1 meter, or $\leq$5 cm of poloidal length which is $<$15% of the total divertor length. The predicted T_e is in stark contrast to our DTS measurements where T_e is about 2 eV throughout the divertor. This level of T_e is able to support through conduction at most 5% of the energy flux we observe in these conditions. The plasma density meanwhile has increased a factor of 5 to $n_e \geq 3 \times 10^{20}$ m^{-3} at the divertor plate and 1×10^{20} m^{-3} near the X point.

Convection of plasma energy at the ion sound speed can account for our observed energy flux during these highly radiative conditions. By assuming the convection terms, the last three terms of the right-hand side of Eq. (1) carry all of the measured energy flux we can solve for the required flow velocity ν using the measured density and temperature profiles. The required Mach number is then determined by dividing the flow velocity, ν, by the ion acoustic speed, $c_S = [Zk(T_e + T_i)/m_i]^{1/2}$, and is plotted in Fig. 3. The ion temperature, T_i, is assumed to equal the electron temperature, T_e, at these divertor parameters. The measured energy transport is satisfied if the plasma flows through the divertor at the ion acoustic speed before slowing as it nears the divertor target. Such an extended region of high plasma flow may follow as a consequence of T_e dropping to ~2 eV, so that the ionization mean free path is large enough (~30 cm) to shift the ionization far upstream near the X point. Simulations with the UEDGE code show [16] such conditions for DIII-D plasmas. The slowing of the plasma flow near the divertor, also seen in the modeling, can be due to charge exchange and collisions with the recycling neutrals. Convection of plasma in the poloidal direction, perhaps due to drifts or instabilities, might also explain much of the energy transport.

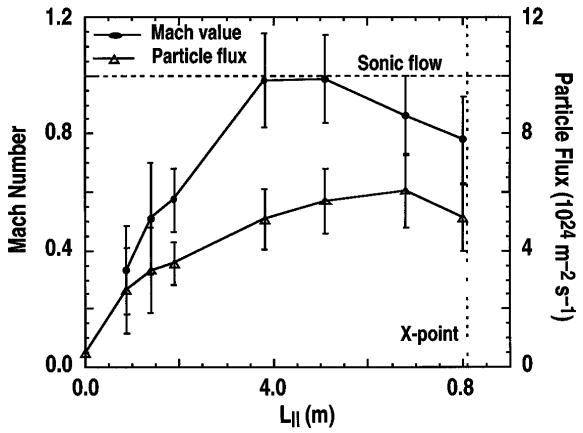

FIG. 3. The flow velocity, in Mach value, required to support the parallel energy flux through convection. Also plotted is the particle flux associated with the flow.

The observed radiation in the divertor is extracted from the plasma thermal energy, through electron excitation, and/or the ionization potential through plasma recombination. To estimate the degree of plasma recombination we convert the inferred parallel plasma flow into particle flux, as plotted in Fig. 3. The uncertainty is large, but the data indicates that about half of the peak particle flux is lost, presumably through recombination, before reaching the divertor target.

Several other physical processes may also contribute to energy transport in the divertor. In treating the SOL as 1D we have neglected perpendicular diffusion which can widen the SOL from the X point to the divertor. We have chosen the width of the SOL as that characteristic at the divertor plate such that any spreading of the SOL from the X point to the divertor due to perpendicular diffusion will result in narrower SOL than assumed in our $q_{\|}$ analysis in Fig. 2. This effect would lead to only a slightly greater T_e needed for conduction dominated transport due to the strong $T_e^{5/2}$ dependence of thermal conductivity. A narrower SOL upstream from the target would also require a greater particle flux in that region than that plotted in Fig. 3. Previous experiments and modeling with UEDGE on DIII-D have shown perpendicular transport to account for $\leq$10% of the transport in the divertor SOL [17].

It is also possible for charge-exchange and ion-neutral collisions to carry away additional energy from the plasma. The bolometer arrays measure any energetic neutrals incident on the detectors. However, bolometers which view the divertor through the ionizing main plasma see the same level of radiation as the side array, indicating that neutrals make up only a small part of our radiated power signal. Neutrals likely do contribute to our measured divertor target heat flux. However, even if all of our target heat flux is due to neutrals this is only about 10% of the total power dissipated in the divertor. Neutrals may also heat the divertor floor outside of the region of the SOL strike point. This represents additional energy loss from the divertor plasma that we do not measure, which in turn may yield a greater $q_{\|}$ upstream than our analysis indicates. The implications of this additional loss are the same as that of perpendicular diffusion as we discussed above. Convection is still needed to explain our observed energy transport.

A non-Maxwellian electron energy distribution might lead to enhanced thermal conduction in the SOL [18]. The hotter less dense SOL plasma above the X point is much less collisional than the divertor plasma. A higher energy collisionless population of electrons may carry a significant fraction of the energy flux from above the X point. The plasma in the divertor and near the X point, however, is very collisional and will thermalize hot electrons very quickly. A 150 eV electron, approximately 4 times the 40 eV thermal T_e of the midplane SOL, will have a slowing distance of $\sim$1 m of parallel length for the divertor plasma of $n_e = 3.0 \times 10^{20}$ and $T_e = 2$ eV. Such an electron should be thermalized within the region of the X point before entering the divertor leg. More work is needed to ascertain the magnitude of the effect on energy transport, but it appears unlikely it can explain our data.

Finally, the edge-localized modes (ELMs) in these ELMing H-mode plasmas may play a role in the power balance of the divertor. ELMs are bursts of energy and particles released into the SOL from the main plasma. They may temporarily heat the SOL and divertor plasma allowing more power to be conducted for a short time. Additional radiation also occurs during the ELM burst. Our diagnostics typically integrate over the ELM period and average their effects. Previous analysis of ELMs on DIII-D [19] has shown that $\leq$10% of the injected power is dissipated in the outboard divertor during the brief ELM pulse. We have measured with fast diagnostics the ELM heat flux and radiation, in the outboard divertor, for plasmas with the same parameters as presented above. The total ELM power represents $\leq$20% of the time-averaged divertor power. Though ELMs may play a role in the dynamic behavior of the divertor they do not account for the power flow observed in the experiment.

High power density tokamaks are expected to have difficulty achieving distributed radiation in the divertor if the energy flux is dominated by electron thermal conduction, since only a very small region of the divertor will have an electron temperature over which neutral deuterium and intrinsic low Z impurities can radiate. Noncoronal effects may allow more radiation at higher T_e, but this effect is expected to be limited [20]. Use of higher Z impurities may increase radiation at higher temperatures, but there are significant limitations to the level of contamination allowed in the main plasma. We have shown in DIII-D that convection can allow transport of energy through the divertor at low temperature enabling the plasma to radiate, recombine, and dissipate the power before deposition on the divertor target. The convective flow is likely created by upstream ionization due to the low T_e and ionization rate in the divertor. This convection allows a much greater dissipation of divertor power than implied by conductive transport. However, for future high power density tokamaks, such as ITER, much work remains to use these concepts in a self-consistent system which is still compatible with high confinement in the main plasma.

This is a report of work supported by the U.S. Department of Energy under Contracts No. DE-AC03-89ER51114 and No. DE-AC05-96OR22464.

*Permanent address: Lawrence Livermore National Laboratory, Livermore, CA 94551-9900.
†Permanent address: Oak Ridge Associated Universities, Oak Ridge, TN 37831.
‡Permanent address: Sandia National Laboratories, Livermore, CA 94551-0969.

[1] G. Janeschitz *et al.*, J. Nucl. Mater. **220–222**, 73 (1995).
[2] K. Lackner *et al.*, Fusion Eng. Des. **22**, 107 (1993).
[3] V. S. Chan *et al.*, in *Proceedings of the 16th IAEA Fusion Energy Conference, Montreal, Canada, 1996* (International Atomic Energy Agency, to be published).
[4] G. Janeschitz *et al.*, in *Proceedings of the 16th IAEA Fusion Energy Conference, Montreal, Canada, 1996* (Ref. [3]).
[5] S. I. Braginskii, in *Reviews of Plasma Physics*, edited by M. A. Leontovich (Consultants Bureau, New York, 1965), Vol. 1, p. 205.
[6] M. A. Mahdavi *et al.*, Phys. Rev. Lett. **47**, 1602 (1981).
[7] D. E. Post *et al.*, J. Nucl. Mater. **121**, 171 (1984).
[8] S. L. Allen *et al.*, J. Nucl. Mater. **196–198**, 804 (1992).
[9] M. J. Schaffer *et al.*, Nucl. Fusion **31**, 1750 (1991).
[10] A. W. Leonard *et al.*, Rev. Sci. Instrum. **66**, 1201 (1995).
[11] D. N. Hill *et al.*, Rev. Sci. Instrum. **59**, 1878 (1988).
[12] T. N. Carlstrom *et al.*, Rev. Sci. Instrum. **68**, 1195 (1997).
[13] S. L. Allen *et al.*, J. Nucl. Mater. (to be published).
[14] P. C. Stangeby *et al.*, Nucl. Fusion **30**, 1225 (1990).
[15] T. W. Petrie *et al.*, Nucl. Fusion **37**, 321 (1997).
[16] G. D. Porter and the DIII-D Team, in *Proceedings of the 23rd European Conference on Controlled Fusion and Plasma Physics, Kiev, Russia, 1996* (Institute of Physics Publishing, Bristol, UK, 1996), Vol. 20C, Part II, p. 699.
[17] G. D. Porter *et al.*, Phys. Plasmas **3**, 1967 (1996).
[18] O. V. Batishchev, "Kinetic Effects in Tokamak Scrape-off Layer Plasmas" (to be published).
[19] A. W. Leonard *et al.*, J. Nucl. Mater. (to be published).
[20] M. A. Mahdavi, J. Nucl. Mater. (to be published).